Enhanced Super-resolution Imaging by Bilayer Aluminum Superlens in DUV Photolithography

Jing WANG

Shanghai Industrial μTechnology Research Institute (SITRI);

School of Microelectronics, Shanghai University

Email: jing_wang@shu.edu.cn

Introduction

- In 2000, Pendry theoretically proposed that [1], a metal planar can be used for imaging beyond diffraction limit, which was then experimentally demonstrated by Zhang et al in 2005 [2].
- Bilayer metal planar superlens has been studied for its superior imaging ability and simple structure, based on approximate effective medium theory (EMT) [3] or 3-layer MIM waveguide theory [4].
- In this poster, the photolithographic system with bilayer Al planar superlens was theoretically investigated to enhance super-resolution imaging performance, based on the five-layer waveguide theory, SPP mode cutoff method, and full-vector FDTD verification.

Single Metallic Superlens

Metallic superlens compensates exponential decay of the evanescent field away from the object by surface plasmons (SP) resonances.

The optical transfer function [5] of the 3-layer insulator-metal-insulator （IMI） system

$$\tau = \tau_1 \cdot \tau_m \cdot \tau_3$$

$$\tau_i = \exp(ik_{zi}d_i), i = 1,3$$

$$\tau_m = \frac{t_0 t_d \exp(ik_{zm}d)}{1 - r_0 r_d \exp(2ik_{zm}d)}$$

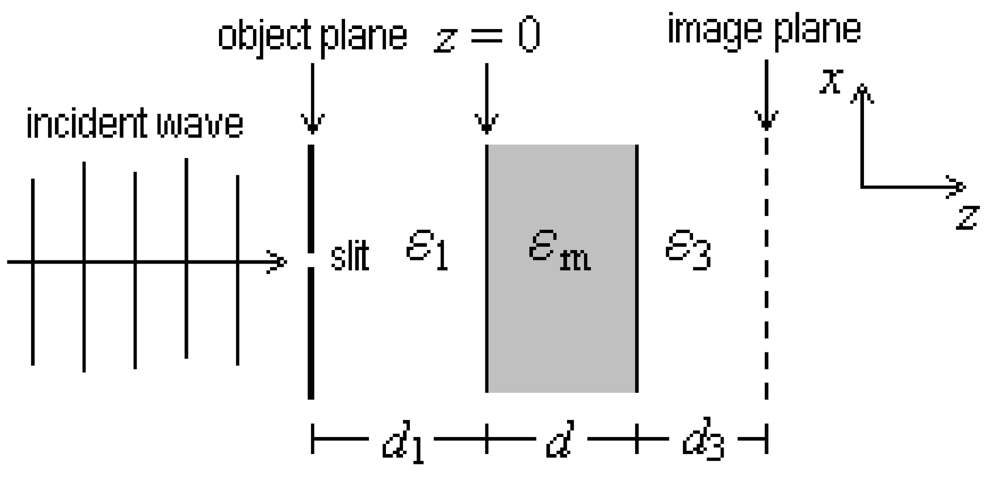

Fig. 1 Near field imaging system with the single metallic superlens

It was known that, typical transfer function of a thin Al superlens contains two amplification peaks, corresponding to two excited SPP modes.

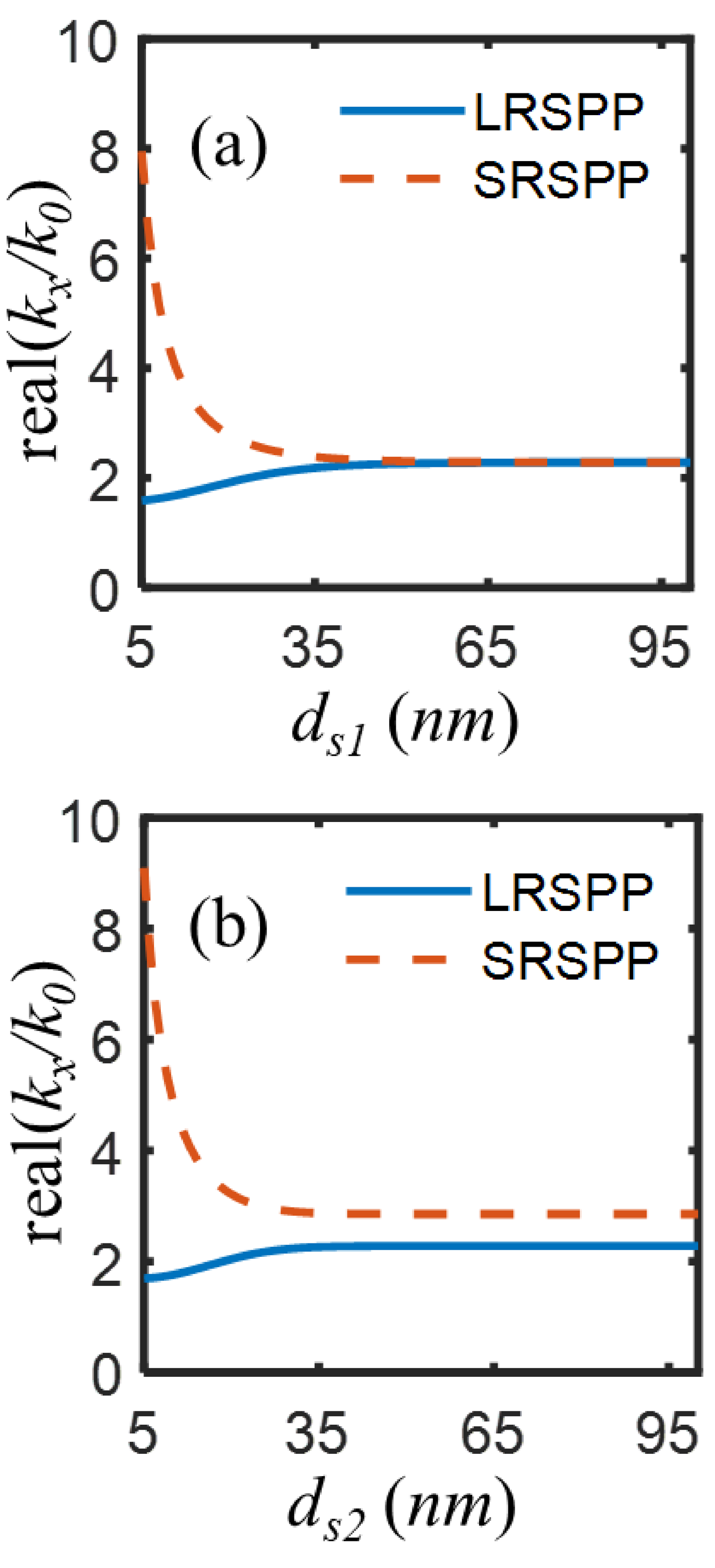

Fig. 2 Real part of effective mode indices of (a) symmetric IMI with ε1=ε3=2.4, and (b) asymmetric IMI with ε1=2.4 and ε3=2.89, for Al superlens of thickness ranging from 5 nm to 100 nm.

Bilayer Metallic Superlens

From the object plane just behind the mask to the imaging plane, the imaging system with bilayer superlens is a finite-thickness metal-insulator-metal（f-MIM） structure, or 5-layer.insulator-metal-insulator-metal-insulator (IMIMI).

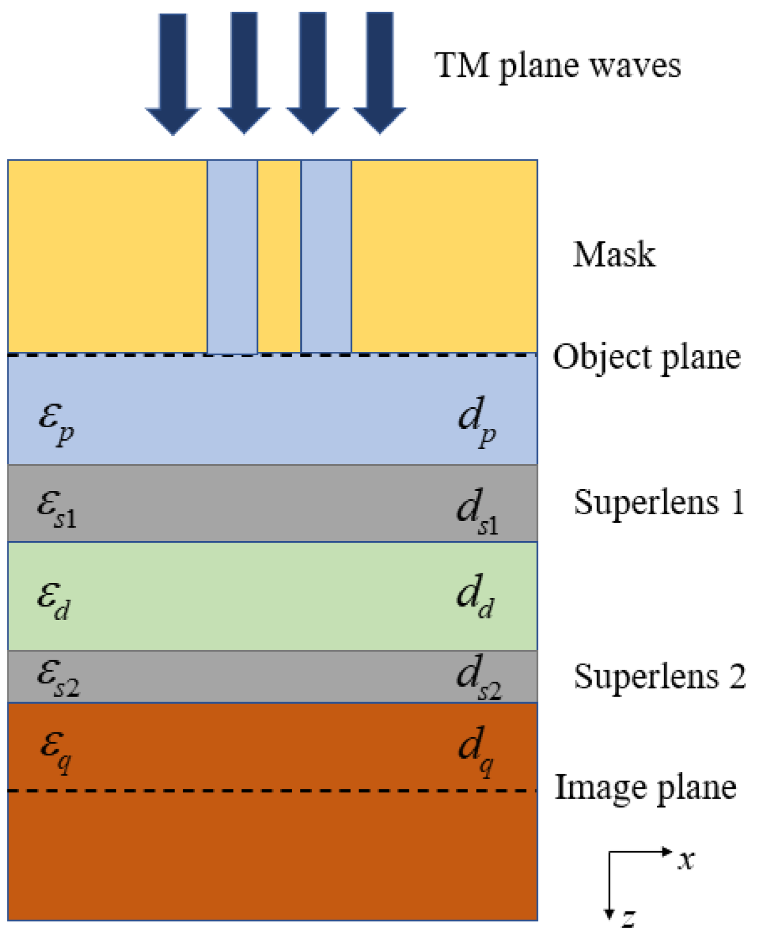

Fig. 3 Near-field photolithographic imaging system of double-layer metal superlens.

Optical transfer function from object plane to image plane:

$$\begin{aligned}
&\tau_{f-MIM} \\
&= \tau_{s1} \cdot \tau_d \cdot \tau_{s2} \\
&= \frac{e_{s1} \cdot t_{p_s1} \cdot t_{s1_d}}{1 - e_{s1}^2 \cdot r_{s1_p} \cdot r_{s1_d}} \\
&\cdot \frac{e_d}{1 - e_d^2 \left(\frac{r_{d_s2} + e_{s2}^2 \cdot r_{s2_q}}{1 - e_{s2}^2 \cdot r_{s2_d} \cdot r_{s2_q}} \right) \left(\frac{r_{d_s1} + e_{s1}^2 \cdot r_{s1_p}}{1 - e_{s1}^2 \cdot r_{s1_p} \cdot r_{s1_d}} \right)} \\
&\cdot \frac{e_{s2} \cdot t_{d_s2} \cdot t_{s2_q}}{1 - e_{s2}^2 \cdot r_{s2_d} \cdot r_{s2_q}}
\end{aligned}$$

Dispersion relation of five-layer waveguide [6]:

$$\begin{aligned}
&e_d^2 \\
&= \left[e_{s2} \left(k_{z_q}/\varepsilon_q - k_{z_s2}/\varepsilon_{s2} \right) \left(k_{z_q}/\varepsilon_q - k_{z_s2}/\varepsilon_{s2} \right) \right. \\
&\left. + e_{s2}^{-1} \left(k_{z_q}/\varepsilon_q + k_{z_s2}/\varepsilon_{s2} \right) \left(k_{z_q}/\varepsilon_q + k_{z_s2}/\varepsilon_{s2} \right) \right] \\
&\cdot \left[e_{s1} \left(k_{z_p}/\varepsilon_p - k_{z_s1}/\varepsilon_{s1} \right) \left(k_{z_s1}/\varepsilon_{s1} - k_{z_d}/\varepsilon_d \right) \right. \\
&\left. + e_{s1}^{-1} \left(k_{z_p}/\varepsilon_p + k_{z_s1}/\varepsilon_{s1} \right) \left(k_{z_s1}/\varepsilon_{s1} + k_{z_d}/\varepsilon_d \right) \right] \\
&/ \left[e_{s2} \left(k_{z_q}/\varepsilon_q - k_{z_s2}/\varepsilon_{s2} \right) \left(k_{z_q}/\varepsilon_q + k_{z_s2}/\varepsilon_{s2} \right) \right. \\
&\left. + e_{s2}^{-1} \left(k_{z_q}/\varepsilon_q + k_{z_s2}/\varepsilon_{s2} \right) \left(k_{z_q}/\varepsilon_q - k_{z_s2}/\varepsilon_{s2} \right) \right] \\
&/ \left[e_{s1} \left(k_{z_p}/\varepsilon_p - k_{z_s1}/\varepsilon_{s1} \right) \left(k_{z_s1}/\varepsilon_{s1} + k_{z_d}/\varepsilon_d \right) \right. \\
&\left. + e_{s1}^{-1} \left(k_{z_p}/\varepsilon_p + k_{z_s1}/\varepsilon_{s1} \right) \left(k_{z_s1}/\varepsilon_{s1} - k_{z_d}/\varepsilon_d \right) \right]
\end{aligned}$$

SPP modes and MTF

IMIMI waveguide could support up to 4 SPP modes, e. g. symmetrically coupled long-range SPP (s-LRSPP), antisymmetrically coupled LRSPP(a-LRSPP), symmetrically coupled short-range SPP (s-SRSPP), and antisymmetrically-coupled SRSPP (a-SRSPP).

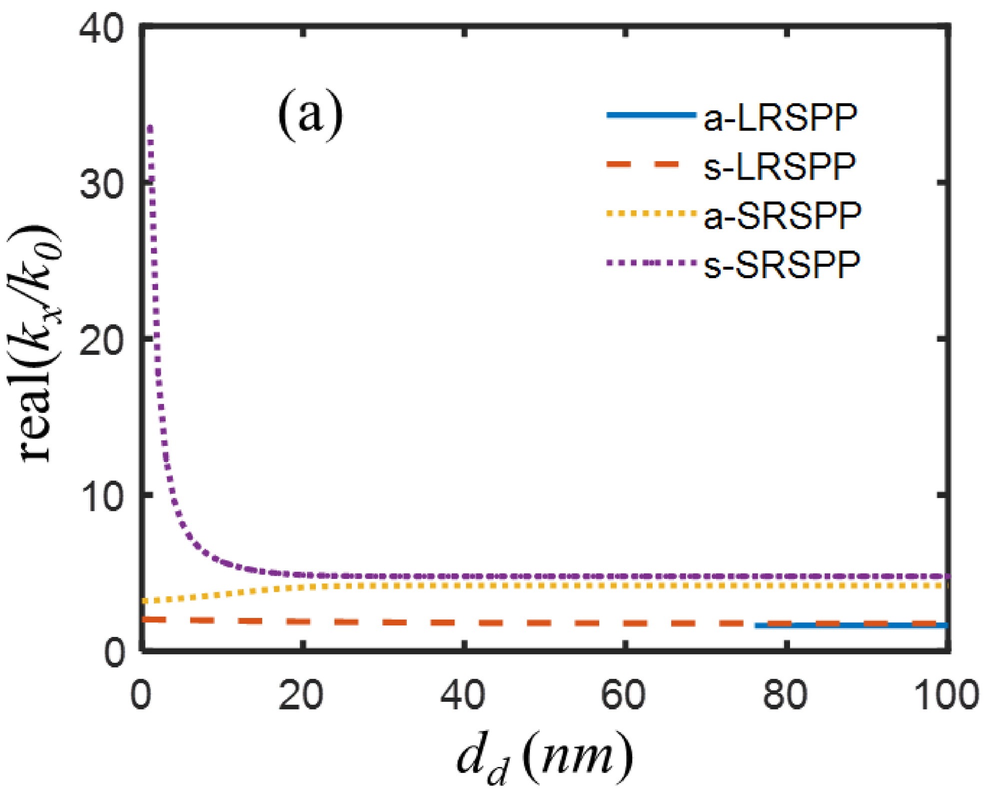

Fig. 4 (a) effective mode indices of a-LRSPP, s-LRSPP, a-SRSPP and s-SRSPP of IMIMI waveguide, and (b) the transmission coefficient of f-MIM waveguide, for two 10nm Al superlenses and a sandwiched SiO2 layer .

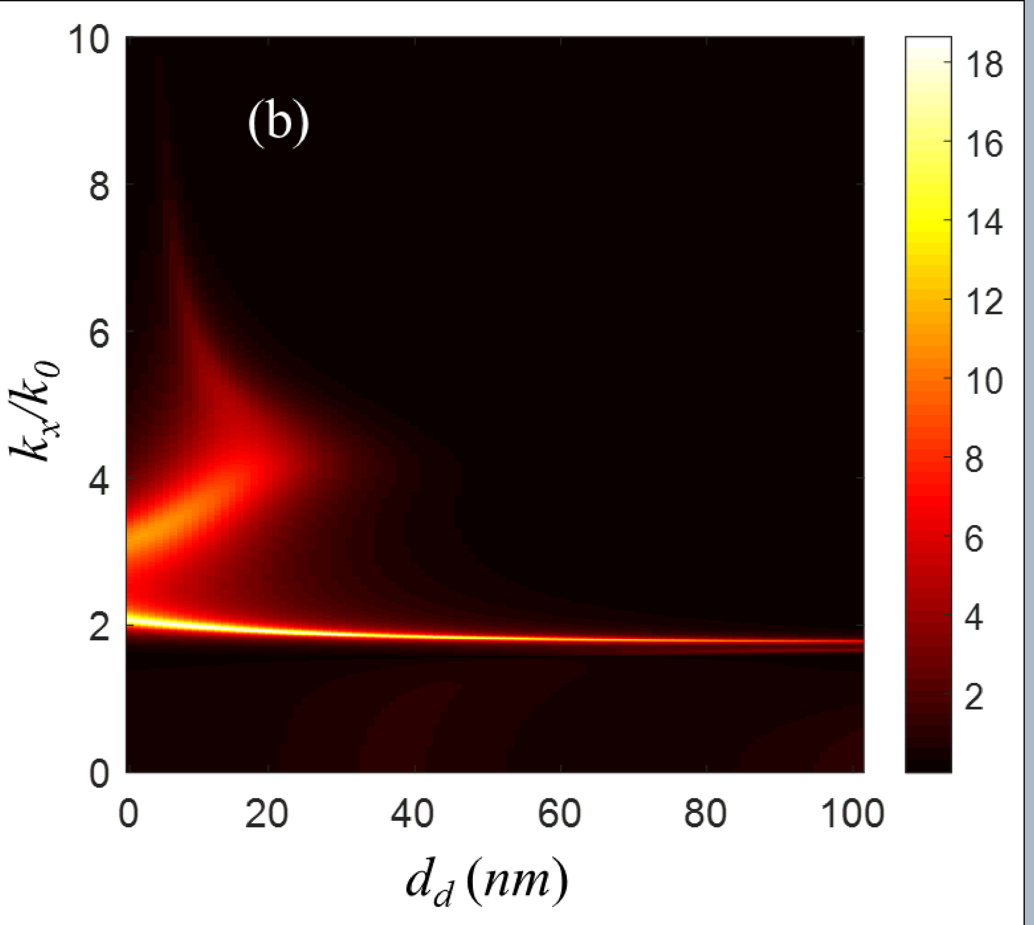

The most remarkable and highest peak, located in proximity to kx/k0=2, was associated with s-LRSPP mode. This amplification would adversely affect super-resolution imaging.

s-LRSPP mode cutoff and FDTD validation

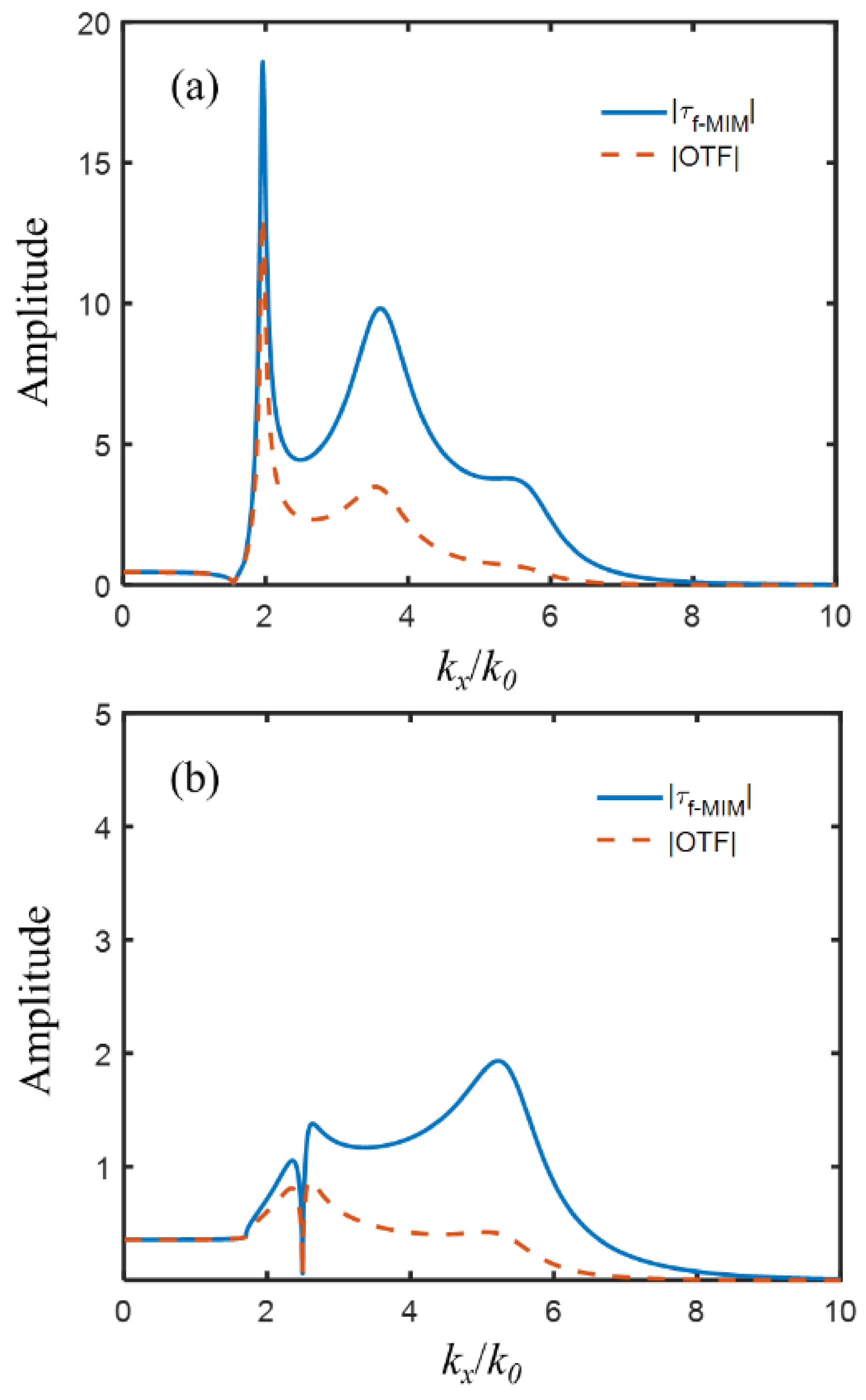

Fig. 5 The MTF (a) before, and (b) after s-LRSPP cutoff.

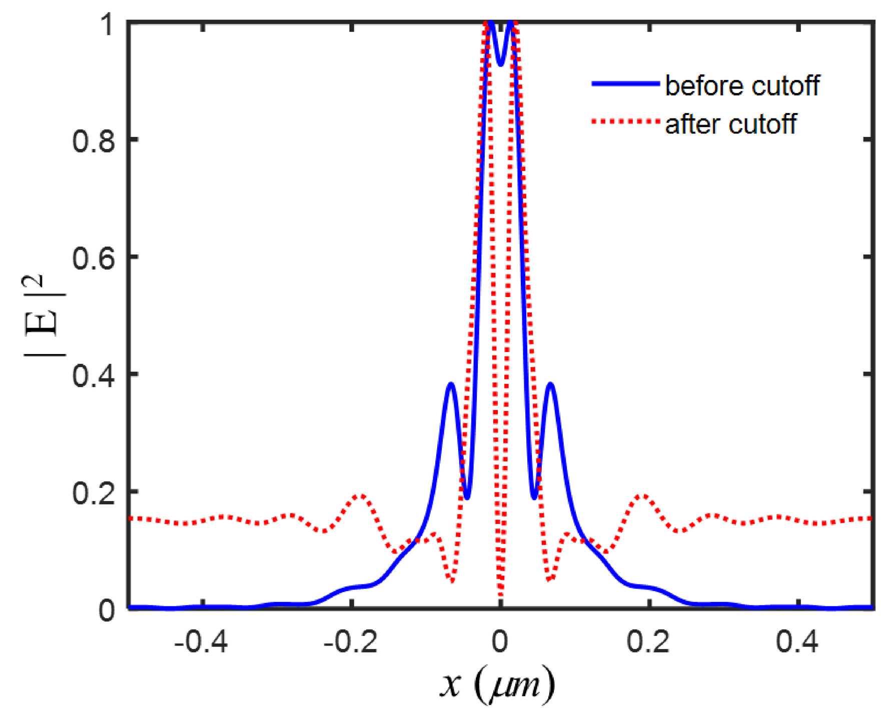

Fig. 6 For W mask of two slits with a slit width 15nm and a spacer width 15nm, the normalized electrical filed intensity (a) before mode cutoff and (b) after mode cutoff, on the image plane by FDTD simulations.

Conclusion

- Intrinsic relation between transfer function of photolithographic imaging system with bilayer Al superlens and SPP modes of IMIMI waveguide.
- Cutoff symmetrically coupled long-range SPP (s-LRSPP) for improving the imaging performance.
- Improved super-resolution imaging performance (two slits with a slit width 15nm and a spacer width 15nm) was verified by full-vector FDTD simulations.

Funding

Shanghai Pujiang Program (20PJ1418600)

Reference

[1] J. B. Pendry, Phys. Rev. Lett. **85**, 3966-3969 (2000).)
[2] N. Fang, H. Lee, C. Sun and X. Zhang, Science, 308, 534-537 (2005)
[3] K. Elsayad and K. G. Heinze, PLoS One, vol. 4, no. 12, 2009
[4] B. Zeng, X. Yang, C. Wang, and X. Luo, Opt Express, vol. 17, no. 19, 2009
[5] G. Tremblay and Y. Sheng, Applied Optics, Vol. 49, No. 7 (2010)
[6] L. Wang, Y. Gu, X. Hu, and Q. Gong, Appl Phys B, vol. 104, no. 4, pp. 919–924, 2011